MULTIFUNCTIONAL 3D PRINTED BATIO$_3$ PLATONIC SOLIDS PACKAGING FOR IMPLANTABLE MICRODEVICES

Sayemul Islam[1], Sumnoon Ahmed[1], Alanis I. Santiago[1], Michael Domic[1], Jungkwun Kim[2], Seung H. Song[3], and Albert Kim[1]*

[1]Department of Electrical and Computer Engineering, Temple University, Philadelphia, PA, USA
[2]Kansas State University, Manhattan, KS, USA
[3]Sookmyung Women's University, Seoul, Korea

ABSTRACT

In this paper, we present a multifunctional packaging technique for implantable microdevices. The packaging is based on 3D printed bulk piezoelectric barium titanate ($BaTiO_3$) ceramic with unique geometrical shapes (i.e., regular convex polyhedrons; Platonic solid). The $BaTiO_3$ ceramic provides not only a seamless packaging for essential electronics but also a power source for those electronics through ultrasonic powering. Ultrasound has been an attractive powering source for many implantable microdevices. However, most ultrasonic receivers are rectangular or disc, not in ideal form factors; ultrasound is often deflected within the path, and the miniature implants might shift and rotate, resulting in an angular misalignment. Tailoring a three-dimensional polyhedral architecture (i.e., Platonic solid) for an mm-scale ultrasonic receiver can dramatically enhance its omnidirectionality. Utilizing the 3D printing technique, we devised a dodecahedron-shaped $BaTiO_3$ ceramic with the center void space for electronics embodiment. As a proof of concept, an LC (inductor-capacitor pair) resonator is implemented as a representative implantable microdevice. When ultrasound impacts the dodecahedron $BaTiO_3$ ultrasonic receiver, it energizes the embedded LC oscillator, generating resonance radio frequency (RF) waves, which can be detected by an external antenna. The demonstrated device with three combinations of an inductor and a 100-pF capacitor show three unique peaks in the RF spectrum at 2.57, 11.51, and 134.33 MHz, respectively.

KEYWORDS

Piezoelectric; Platonic solids; 3D packaging; implantable microdevice.

INTRODUCTION

Implantable medical devices (IMDs) are useful in monitoring complex physiological information, performing actuation, or drug delivery [1]. Millions of patients have been receiving some form of IMDs each year to improve their quality of life since the placement of the first implantable pacemaker in 1958 [2]. Some examples of implantable medical devices other than cardiac pacemakers are cochlear implants, neurostimulators, drug infusion pumps, implantable insulin pumps, etc. Most of these devices need a continuous source of power for their operation, and most of the time, it is provided using internal batteries. Typical consumption can vary from 30 μW to 10 mW depending on the type of the IMDs [3] However, the use of batteries may not be wise when the implant is considerably small and requires a long-term operation. Therefore, remote powering is considered in many of IMDs.

Among many remote powering technologies, RF or inductive powering is the most well-known. However, the RF powering is prone to high attenuation for deep tissue implants, especially at higher frequencies. The inductive powering also suffers from a short operating range and misalignment issues. As an alternative and promising remote powering method, ultrasound is extensively discussed due to its effective power transfer into deep tissue implants [4]–[8]. Furthermore, ultrasonic powering is less susceptible to directionality, especially the angular misalignment between the transmitter and the receiver transducer. Also, even if IMDs are placed out of optimal location and lose efficiency, some steps can be taken to counter that effect. For example, we previously demonstrated omnidirectional ultrasonic powering for millimeter-scale implantable devices by employing symmetricity of cuboids form factor [9]. Although the transducers typically used in IMDs, usually utilize manufactured lead zirconate titanate (PZT) ceramic, it is possible to make custom 3D printed shapes of piezoelectric transducers that provide a higher degree of symmetricity using lead-free ferroelectric $BaTiO_3$ nanoparticles.

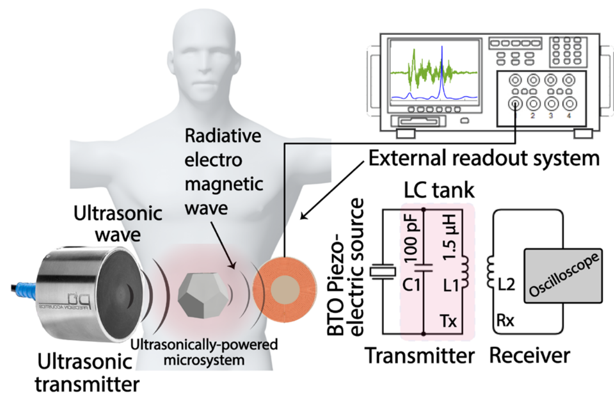

Figure 1: Implantable 3D printed and packaged microdevice sending information through RF radiation by using ultrasonic interrogation.

Here, we present a 3D printed, highly symmetric, piezoelectric transducer as an ultrasonic powering receiver. The transducer also has a small, voided space for carrying small electronics. We previously reported that the ultrasonic powering efficiency and omnidirectionality could be improved when various polyhedral Platonic solids (cube, octahedron, dodecahedron, sphere) are employed as a receiver [10]. Notably, the dodecahedron shape showed a minimal effect on the directionality compared to others. Therefore, we implemented a 3D printed dodecahedron-shaped piezoelectric transducer using $BaTiO_3$ as packaging for an LC resonator. The LC resonator has been utilized in many physiological sensors by employing either a capacitive or inductive sensor [11], [12]. Fig. 1 shows the schematic view of the proposed microdevice. The implanted Platonic solid ultrasonic receiver converts incoming ultrasound from the external transmitter to electrical power for the embedded LC resonator (not shown). The LC resonator then propagates an RF signal in a specific frequency that contains physiological information, picked up wirelessly by a readout system.

MATERIALS AND METHODS

Fig. 2 shows the fabrication process. The fabrication methodology was inspired by the recent work of Kim et al. [13]. First, the polyvinylidene difluoride (PVDF; Alfa Aesar, USA) was dissolved in N, N' dimethylformamide (DMF; Thermo Scientific, USA) with a 1:8.8 wt.% ratio while heated in a water bath at 80°C (Fig. 2a). The $BaTiO_3$ nanoparticles (500 nm; US research nanomaterials, USA) were then thoroughly and uniformly mixed (ratio 3.345:1) with the binder solution (PVDF + DMF) for at least 5 minutes using a stirrer (Fig. 2b). The mixture was then loaded into an extrusion syringe pump (10 mL, 600 µm nozzle) and used to 3D print a bespoke form (i.e., dodecahedron with radius = 5.5 mm and a 3.5 mm diameter hole) (Fig. 2c). The 3D printed dodecahedron was then baked in an oven (AT09p7.110 Ai, Across International) for 2 hours at 120°C to evaporate DMF completely (Fig. 2d). Then, the samples were placed in a tube furnace (GSL 1600X, MTI Corporation, USA) for debinding at 650°C for 1 hour, followed by sintering at 1190°C for 3 hours (Fig. 2e). The ramp-up and ramp-down temperature rates were maintained at 5°C/min. After sintering, a conductive electrode layer was created inside the hole and outside using commercially available conductive silver epoxy (8331D, MG Chemicals).

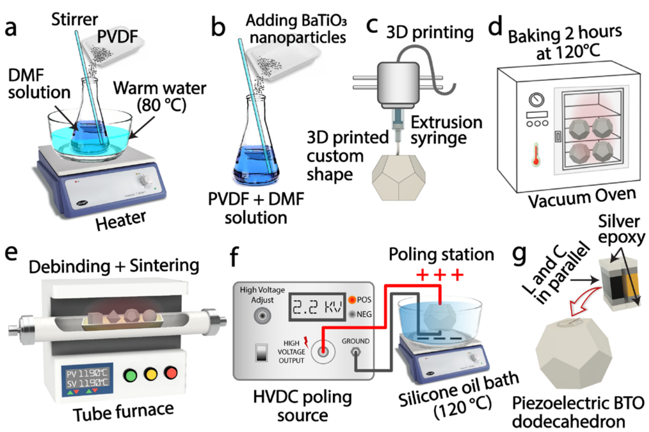

Figure 2: The fabrication process of implantable microdevices.

Since the electric dipoles in bulk $BaTiO_3$ dodecahedron were randomly oriented, they needed to be poled using a high voltage (V_{poling} > 1kV/mm) (Fig. 2f). For the polling process, the samples were placed in a custom-made poling stage which was submerged in silicone oil heated above curie temperature (120°C) [14] and connected to a high voltage DC power supply (230-30R, Spellman, USA) using spring-loaded connectors at the bottom and the top electrodes. They were poled at a high voltage (1 kV/mm) for 1 hour to activate piezoelectricity by aligning randomly oriented electric dipoles. After poling, a pair of an unshielded inductor and a capacitor were soldered into the void space, making contact with the inside electrode (Fig. 2g). The opposite terminal of the LC resonator was then connected to the outer electrode using wire and silver epoxy. Finally, the electrical connections were secured using biocompatible resin (BioMed Clear, Formlabs).

Fig. 3 shows the different states of the $BaTiO_3$ material during the process. Initially, the $BaTiO_3$ was in a dry powdered state. The addition of binder materials (PVDF + DMF) helped to retain the custom shape when molded or 3D printed. Fig. 3(d) shows a scanning electron microscopic (Quanta 450 FEG) image of $BaTiO_3$ before the debinding and sintering process. The particles can be seen attached to each other due to the binding materials. Drying the sample at this state causes the DMF to evaporate and still maintains the shape. After the debinding and the sintering process, the PVDF evaporated out, leaving only $BaTiO_3$ nanoparticles. During the sintering, $BaTiO_3$ particles fused with each other, forming a large and bulk $BaTiO_3$ sample, as shown in Fig. 3(e). The SEM images were taken with an accelerating voltage of 20 kV, spot size 5.5, ETD (Everhart Thornley Detector) with 2500x magnification, and 166 µm horizontal field width view.

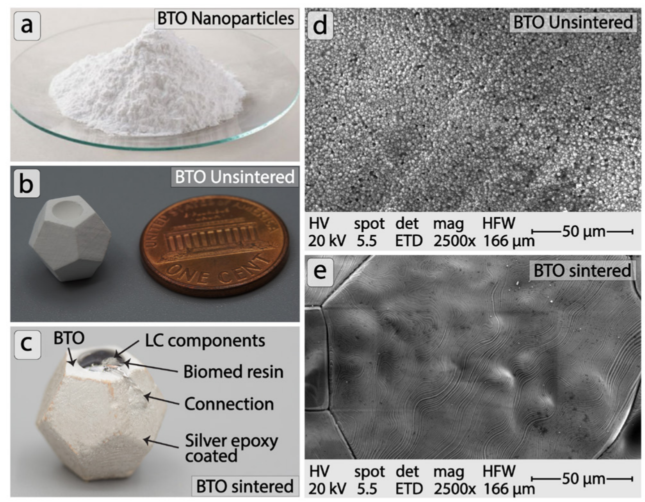

Figure 3: (a) $BaTiO_3$ NPs, (b) sintered $BaTiO_3$, (c) electronics integrated and packaged into the microdevice, (d) SEM pictures of pre-sintered, and (e) sintered $BaTiO_3$ sample.

EXPERIMENT SETUP

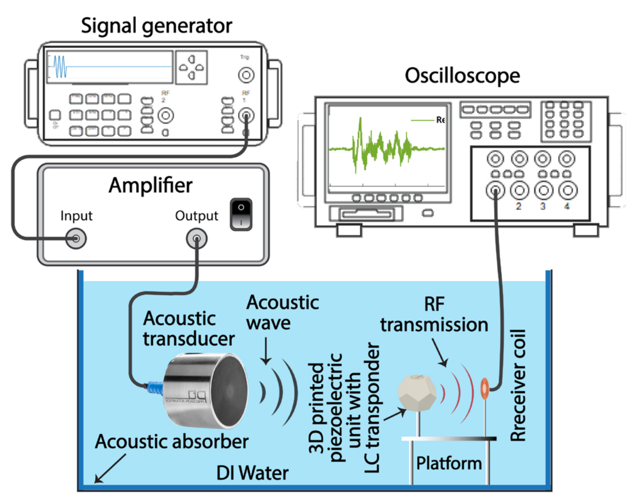

Figure 4: Experiment setup showing the interrogation technique.

The experiment setup is shown in Fig. 4. A water tank (60 × 30 × 40 cm^3) with deionized water was used to mimic the acoustic impedance in the biological environment (acoustic impedance in water is 1.483 MRayls) [15]. Acoustic absorbers were used on the side walls to prevent acoustic reflections and to minimize noise during the experiment. A submersible 60 mm focused acoustic transducer (PA1469, Precision Acoustics Ltd., UK) was used as a transmitter to transmit the acoustic waves to the dodecahedron $BaTiO_3$ ultrasonic receiver with an LC transponder. The transducer was connected to a signal generator (4065, B&K Precision, USA) via an amplifier (1040L, E&I, USA) and driven using a sinusoidal tone burst (N = 5) of amplitude 200 mV (before 55 dB amplification) and a frequency of 670 kHz at 10 ms interval. The average electric power used by the transmitter was only 4 watts. The microdevice was placed directly in the line of sight with the transmitter at a 7.5 cm distance. A receiver coil (dia = 17.8 mm, width = 0.6 mm, turns = 32, layers = 4) was placed 1 cm away from the microdevice to capture the RF transmission. The receiver coil was connected to an oscilloscope (MSO54, Tektronix, Inc.) for displaying and logging the frequency spectrum. Note that a more user-friendly interface with additional descriptive information on the display can be developed for medical professionals in the future.

RESULTS

A. Ultrasonic response and LC oscillation

The ultrasonic transmitter was excited by the signal generator to transmit energy to the microdevice. As the transmitter started energizing, the burst ultrasonic waves could reach the microdevice and induce an electrical power in response to the piezoelectric $BaTiO_3$ transducer. The input wave is shown in Fig. 5(a) and the corresponding piezoresponse is shown in Fig. 5(b). The piezoresponse energizes the LC circuit, which induces oscillation at its resonance frequency until it is gradually damped out due to the energy dissipation in the circuit. The LC oscillation is shown in Fig. 5(c). It can be observed that the LC oscillation (at its resonance) occurred between each cycle of the burst generated by the $BaTiO_3$ transducer. The LC resonator radiated its signal through the unshielded inductor (acting as an antenna) and can be observed using an external antenna. Repetitive input ultrasound bursts were needed to maintain the oscillation and successful signal capture using the receiver coil.

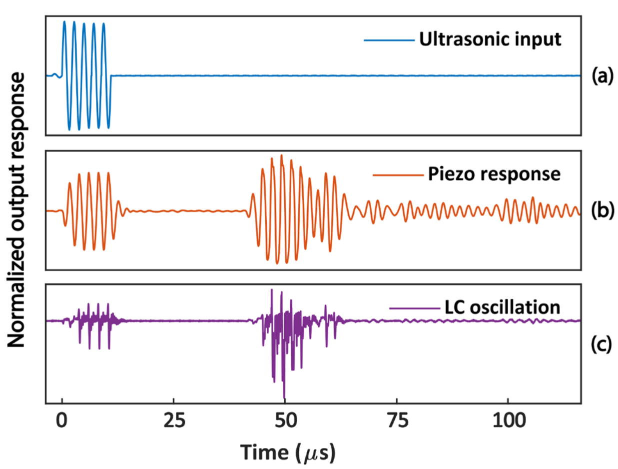

Figure 5: (a) Ultrasonic excitation, (b) piezoelectric response from BTO sample, and (c) oscillation in the LC circuit due to the excitation.

B. Received signal through RF

Three LC resonators with different resonant frequencies were prepared by adjusting inductor values while keeping the capacitor same (C = 100 pF). Three inductor values were 15 nH, 1.5 μH, and 100 μH with corresponding LC resonances at 129.95 MHz, 12.99 MHz, and 1.59 MHz. The transmitted RF signals were observed using the receiver coil on the oscilloscope. The combined frequency spectrum of the wirelessly received signals is shown in Fig. 6. As seen, resonant peaks distinctively appeared as expected with corresponding to the LC resonator circuit combinations. Different inductance values changed the peak location in the spectrum, which demonstrates a good agreement with the calculated resonance values shown in Table 1. The captured waveform carried multiple frequency information: the ultrasonic frequency, ultrasonic bursts frequency, $BaTiO_3$ mechanical resonant frequency, and the LC resonator frequency. To isolate and remove the effect of unwanted signals, we scanned from 1 MHz to 160 MHz in the frequency domain.

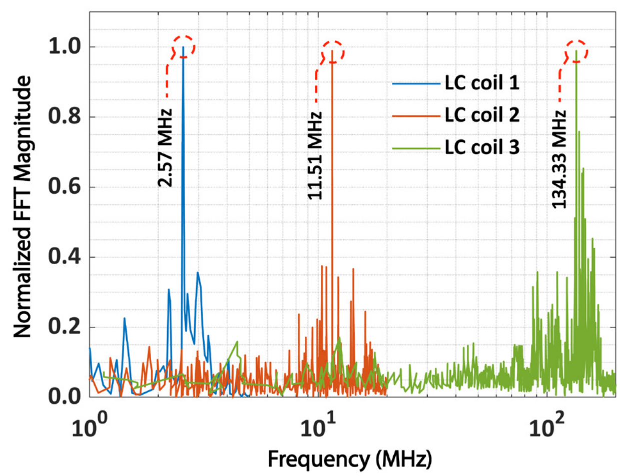

Figure 6: Received RF peaks identified for three different LC combinations.

Table 1: LC tank parameters and corresponding peaks

Parameter	LC type - 1	LC type - 2	LC type - 3
Dimension	L = 1.1 mm W = 1.0 mm	L = 1.1 mm W = 1.0 mm	L = 1.1 mm W = 1.0 mm
Inductance	100 μH	1.5 μH	15 nH
Capacitance	100 pF	100 pF	100 pF
Calculated resonance	1.59 MHz	12.99 MHz	129.95 MHz
Experimental values received	2.57 MHz	11.51 MHz	134.33 MHz

CONCLUSION

The design and fabrication of a multifunctional 3D printed $BaTiO_3$ dodecahedron piezoelectric transducer are demonstrated to be used as packaging for implantable microdevices. As a proof of concept, LC transponders were packaged inside of the transducer. Upon the ultrasonic input, the microdevice could generate and transmit RF signals with peaks indicating the corresponding variable (or sensing) element (inductor in this case). Such multifunctional packaging techniques and advanced miniature electronics are expected to bring numerous biomedical applications in smaller spaces, such as closed-loop sensing and actuation, multi microdevice communication, and enhanced security of the transmitted signal. Therefore, the reported packaging technique shows promising potential in replacing battery-powered or other passive implantable microdevices.

ACKNOWLEDGEMENT

The authors would like to acknowledge Dr. Dmitriy A. Dikin, and Long Zhu from Temple University for their help with the SEM imaging.

Funding: This work was supported by the National Science Foundation (NSF): CAREER award (ECCS-2143723) as well as ECCS-2029077, CNS-2129659, and ECCS-2054567.

CONTACT

For more information, please contact Dr. Albert Kim, email: albertkim@temple.edu; phone: +1 (215) 204-3222.

REFERENCES

[1] W. Khan, E. Muntimadugu, M. Jaffe, and A. J. Domb, “Implantable Medical Devices,” in *Focal Controlled Drug Delivery*, 2014, pp. 33–59.

[2] N. M. van Hemel and E. E. van der Wall, “8 October 1958, D Day for the implantable pacemaker,” *Neth. Heart J.*, vol. 16, no. 1, pp. 3–4, 2008, [Online]. Available: https://www.ncbi.nlm.nih.gov/pmc/articles/PMC2572009/.

[3] X. Wei and J. Liu, “Power sources and electrical recharging strategies for implantable medical devices,” *Front. Energy Power Eng. China*, vol. 2, no. 1, pp. 1–13, 2008, doi: 10.1007/s11708-008-0016-3.

[4] P. J. Larson and B. C. Towe, “Miniature ultrasonically powered wireless nerve cuff stimulator,” *2011 5th Int. IEEE/EMBS Conf. Neural Eng. NER 2011*, pp. 265–268, 2011, doi: 10.1109/NER.2011.5910538.

[5] S. Islam and A. Kim, “An ultrasonically powered active stent for endovascular diseases,” in *2018 Solid-State Sensors, Actuators and Microsystems Workshop, Hilton Head 2018*, May 2018, no. 18, pp. 228–229, doi: 10.31438/trf.hh2018.64.

[6] A. K. Majumdar, S. Islam, and A. Kim, “An ultrasonically powered implantable micro electrolytic ablation (IMEA) for tumor necrosis,” in *2018 Solid-State Sensors, Actuators and Microsystems Workshop, Hilton Head 2018*, May 2018, pp. 100–101, doi: 10.31438/trf.hh2018.29.

[7] A. Kim *et al.*, “An Implantable Ultrasonically-Powered Micro-Light-Source (µLight) for Photodynamic Therapy,” *Sci. Rep.*, vol. 9, no. 1, p. 1395, Dec. 2019, doi: 10.1038/s41598-019-38554-2.

[8] R. Campbell *et al.*, “Implantable Cisplatin Synthesis Microdevice for Regional Chemotherapy,” *Adv. Healthc. Mater.*, vol. 10, no. 3, p. 2001582, Dec. 2021, doi: 10.1002/adhm.202001582.

[9] S. H. Song, A. Kim, and B. Ziaie, “Omnidirectional Ultrasonic Powering for Millimeter-Scale Implantable Devices,” *IEEE Trans. Biomed. Eng.*, vol. 62, no. 11, pp. 2717–2723, Nov. 2015, doi: 10.1109/TBME.2015.2444854.

[10] S. Islam, M. Park, S. H. Song, and A. Kim, “OMNIDIRECTIONAL POLYHEDRAL ULTRASOUND TRANSDUCER FOR POWERING IMPLANTABLE MICRODEVICES,” in *2021 21st International Conference on Solid-State Sensors, Actuators and Microsystems (Transducers)*, Jun. 2021, pp. 1404–1407, doi: 10.1109/Transducers50396.2021.9495556.

[11] M. Lei, A. Baldi, E. Nuxoll, R. A. Siegel, and B. Ziaie, “Hydrogel-based microsensors for wireless chemical monitoring,” *Biomed. Microdevices*, vol. 11, no. 3, pp. 529–538, Jun. 2009, doi: 10.1007/s10544-008-9168-5.

[12] A. Kim, C. R. Powell, and B. Ziaie, “An implantable pressure sensing system with electromechanical interrogation scheme,” *IEEE Trans. Biomed. Eng.*, vol. 61, no. 7, pp. 2209–2217, 2014, doi: 10.1109/TBME.2014.2318023.

[13] H. Kim *et al.*, “Fabrication of bulk piezoelectric and dielectric $BaTiO_3$ ceramics using paste extrusion 3D printing technique,” *J. Am. Ceram. Soc.*, vol. 102, no. 6, pp. 3685–3694, Jun. 2019, doi: 10.1111/jace.16242.

[14] A. Ibrahim, M. Meng, and M. Kiani, “A Comprehensive Comparative Study on Inductive and Ultrasonic Wireless Power Transmission to Biomedical Implants,” *IEEE Sens. J.*, vol. 18, no. 9, pp. 3813–3826, May 2018, doi: 10.1109/JSEN.2018.2812420.

[15] P. Chen *et al.*, “Acoustic characterization of tissue-mimicking materials for ultrasound perfusion imaging research,” *Ultrasound Med. Biol.*, vol. 48, no. 1, pp. 124–142, Jan. 2022, doi: 10.1016/j.ultrasmedbio.2021.09.004.